Electronic Supplementary Material (ESI) for Integrative Biology.

SUPPLEMENTAL MATERIAL:

A computational analysis of pro-angiogenic therapies for peripheral artery disease

Supplemental Figures

Fig S1. Detailed response to biomaterial-based delivery of engineered VEGF constructs to the PAD Calf Muscle.

Fig S2. Efficacy of biomaterial-based VEGF delivery does not depend on endogenous VEGF splicing.

Fig S3. Detailed response to varying doses of "Covalent VEGF with Proteolysis" construct to the PAD Calf Muscle.

Fig S4. Additional metrics of response to gene therapy at Day 6 following treatment.

Fig S5. Detailed time-course response to gene therapy strategies.

Fig S6. Analysis of predicted $VEGF_{165a}$ and $VEGF_{165b}$ distribution in human body following VEGF-targeted antibody therapy.

Fig S7. Effect of VEGF-targeting antibodies on systemic free VEGF distribution.

Fig S8. Additional effects of VEGF-targeting antibodies on endothelial VEGFR2 signaling *in vivo*.

Fig S9. Effects of VEGF-targeting antibodies on endothelial total VEGFR2 ligation *in vivo*.

Fig S10. Effects of VEGF-targeting antibodies on endothelial cell surface VEGFR2 ligation *in vivo*.

Fig S11. Effects of VEGF-targeting antibodies on endothelial cell surface VEGFR1 ligation *in vivo*.

Fig S12. Relative antibody binding to $VEGF_{165a}$ and $VEGF_{165b}$ in the Main Body Mass and PAD Calf Muscle.

Fig S13. Comparison of VEGFR2 activation following biomaterial-based protein delivery, gene therapy, or anti-VEGF treatment.

Supplemental References

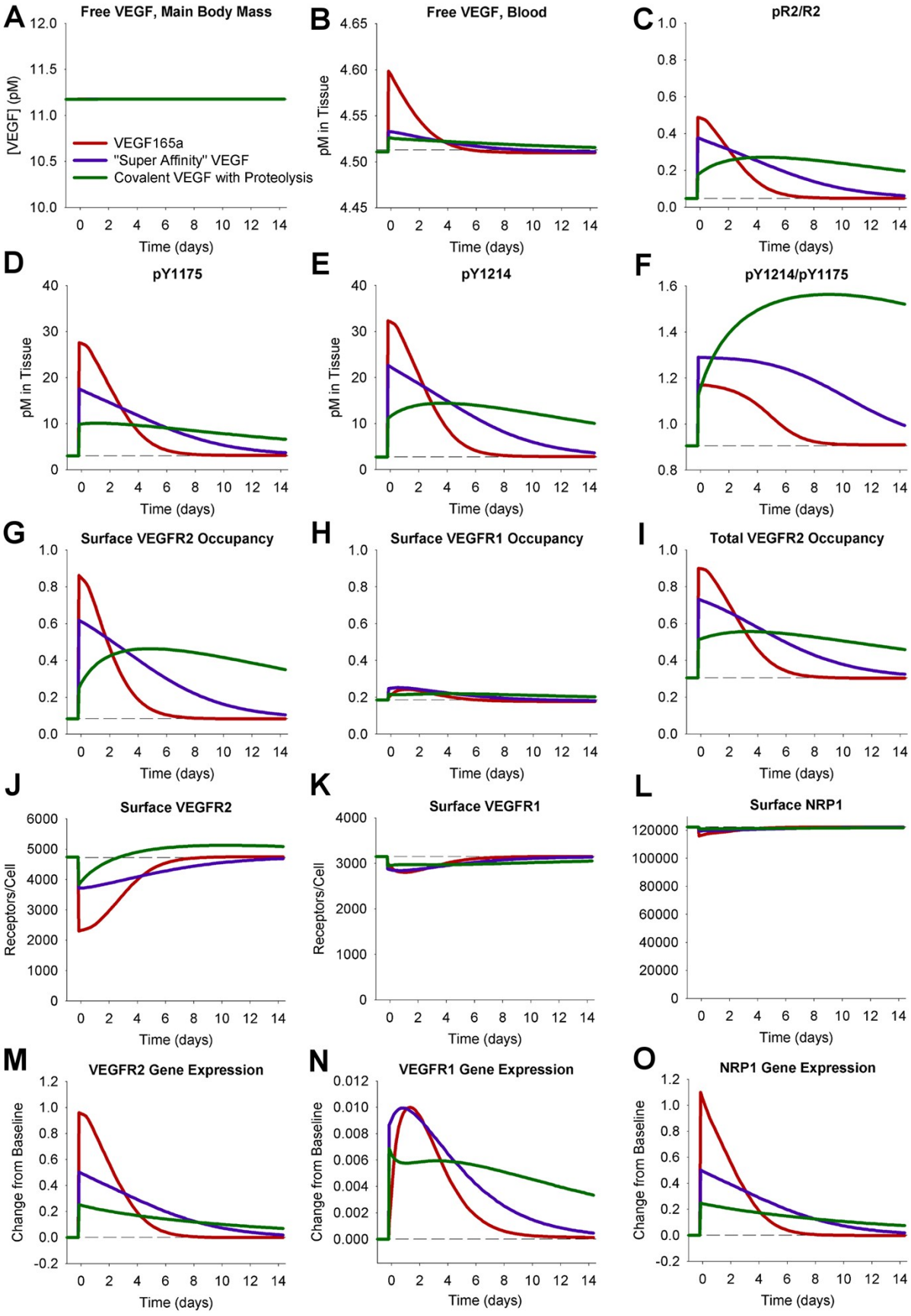
A
Free VEGF, Main Body Mass
[VEGF] (pM)
VEGF165a
"Super Affinity" VEGF
Covalent VEGF with Proteolysis
Time (days)
B
Free VEGF, Blood
pM in Tissue
Time (days)
C
pR2/R2
Time (days)
D
pY1175
pM in Tissue
Time (days)
E
pY1214
pM in Tissue
Time (days)
F
pY1214/pY1175
Time (days)
G
Surface VEGFR2 Occupancy
Time (days)
H
Surface VEGFR1 Occupancy
Time (days)
I
Total VEGFR2 Occupancy
Time (days)
J
Surface VEGFR2
Receptors/Cell
Time (days)
K
Surface VEGFR1
Receptors/Cell
Time (days)
L
Surface NRP1
Time (days)
M
VEGFR2 Gene Expression
Change from Baseline
Time (days)
N
VEGFR1 Gene Expression
Change from Baseline
Time (days)
O
NRP1 Gene Expression
Change from Baseline
Time (days)

Fig S1. Detailed response to biomaterial-based delivery of engineered VEGF constructs to the PAD Calf Muscle. This figure is related to **Fig. 2** of the main manuscript. Free VEGF levels in other compartments (**A-B**), details of VEGFR2 phosphorylation (**C-F**), endothelial receptor occupancy (**G-I**), changes in surface receptor levels following treatment (**J-L**), and the dynamic changes in receptor production required to hold total receptor levels constant following treatment (**M-O**).

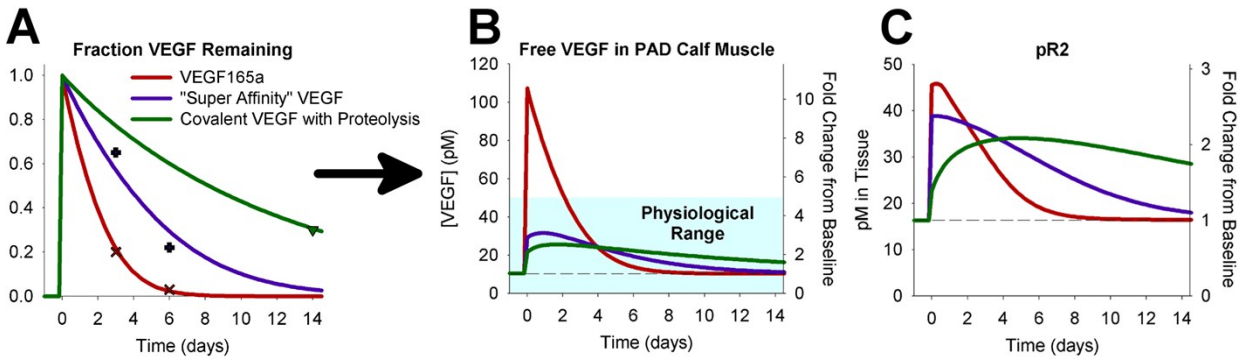

Fig S2. Efficacy of biomaterial-based VEGF delivery does not depend on endogenous VEGF splicing. This figure is related to **Fig. 2** of the main manuscript. Simulations of VEGF release from biomaterial **(A)**, free VEGF in the PAD Calf Muscle **(B)**, and VEGFR2 phosphorylation **(C)**, with no endogenous secretion of $VEGF_{165b}$ (0%, all $VEGF_{165a}$), as opposed to the case shown in **Fig. 2B**, with all $VEGF_{165b}$ (100%). All other conditions and dose size are the same as in **Fig. 2B**. Teal box indicates physiological range of VEGF expression, which typically varies no more than 3-5x in physiological and pathological conditions[1].

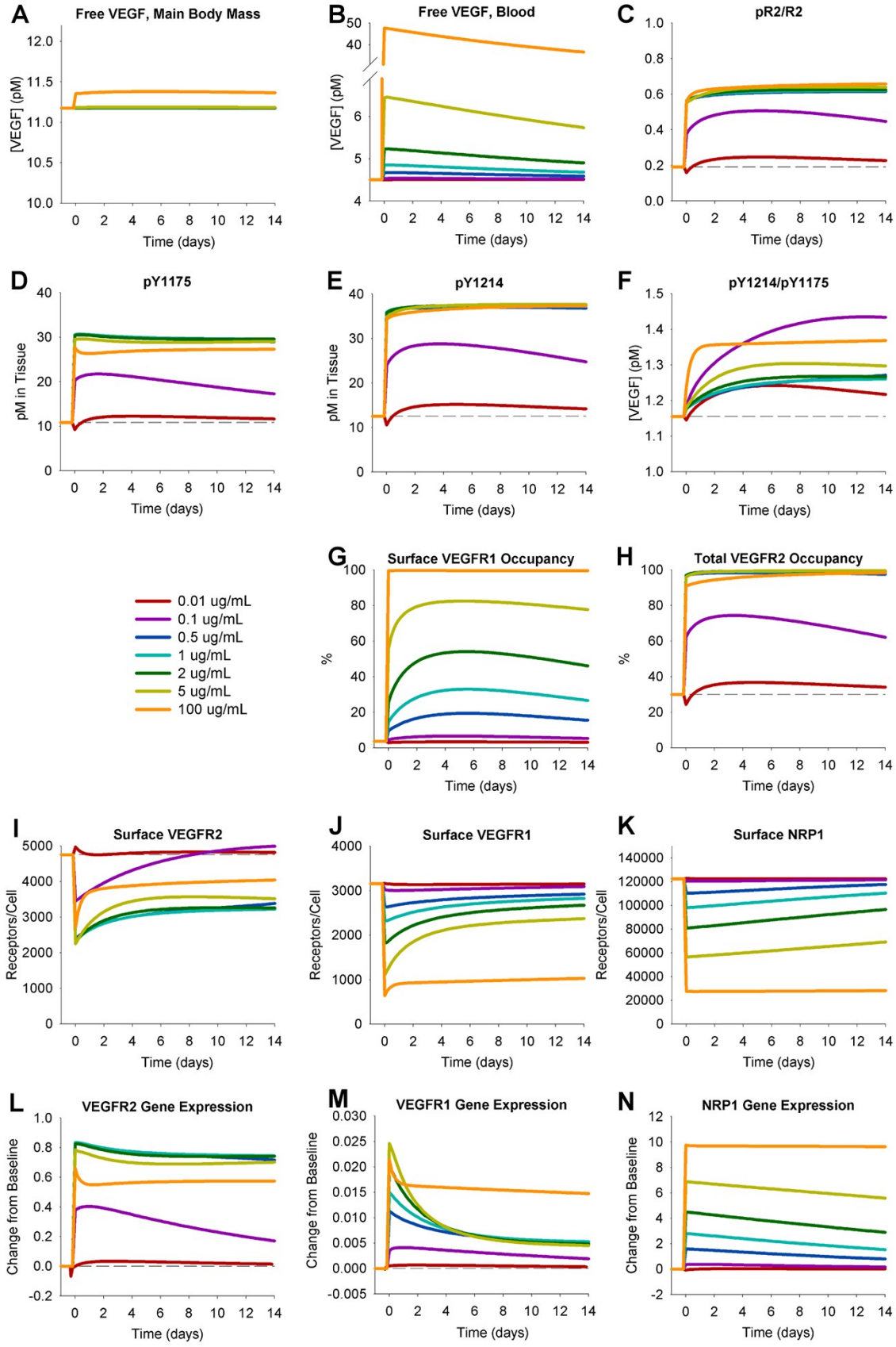
A
Free VEGF, Main Body Mass
[VEGF] (pM)
Time (days)
B
Free VEGF, Blood
[VEGF] (pM)
Time (days)
C
pR2/R2
Time (days)
D
pY1175
pM in Tissue
Time (days)
E
pY1214
pM in Tissue
Time (days)
F
pY1214/pY1175
[VEGF] (pM)
Time (days)
0.01 ug/mL
0.1 ug/mL
0.5 ug/mL
1 ug/mL
2 ug/mL
5 ug/mL
100 ug/mL
G
Surface VEGFR1 Occupancy
%
Time (days)
H
Total VEGFR2 Occupancy
%
Time (days)
I
Surface VEGFR2
Receptors/Cell
Time (days)
J
Surface VEGFR1
Receptors/Cell
Time (days)
K
Surface NRP1
Receptors/Cell
Time (days)
L
VEGFR2 Gene Expression
Change from Baseline
Time (days)
M
VEGFR1 Gene Expression
Change from Baseline
Time (days)
N
NRP1 Gene Expression
Change from Baseline
Time (days)

Fig S3. Detailed response to varying doses of "Covalent VEGF with Proteolysis" construct to the PAD Calf Muscle. This figure is related to **Fig. 2** of the main manuscript. Free VEGF levels in other compartments (**A-B**), details of VEGFR2 phosphorylation (**C-F**), endothelial receptor occupancy (**G-H**), changes in surface receptor levels following treatment (**I-K**), and the dynamic changes in receptor production required to hold total receptor levels constant following treatment (**L-N**).

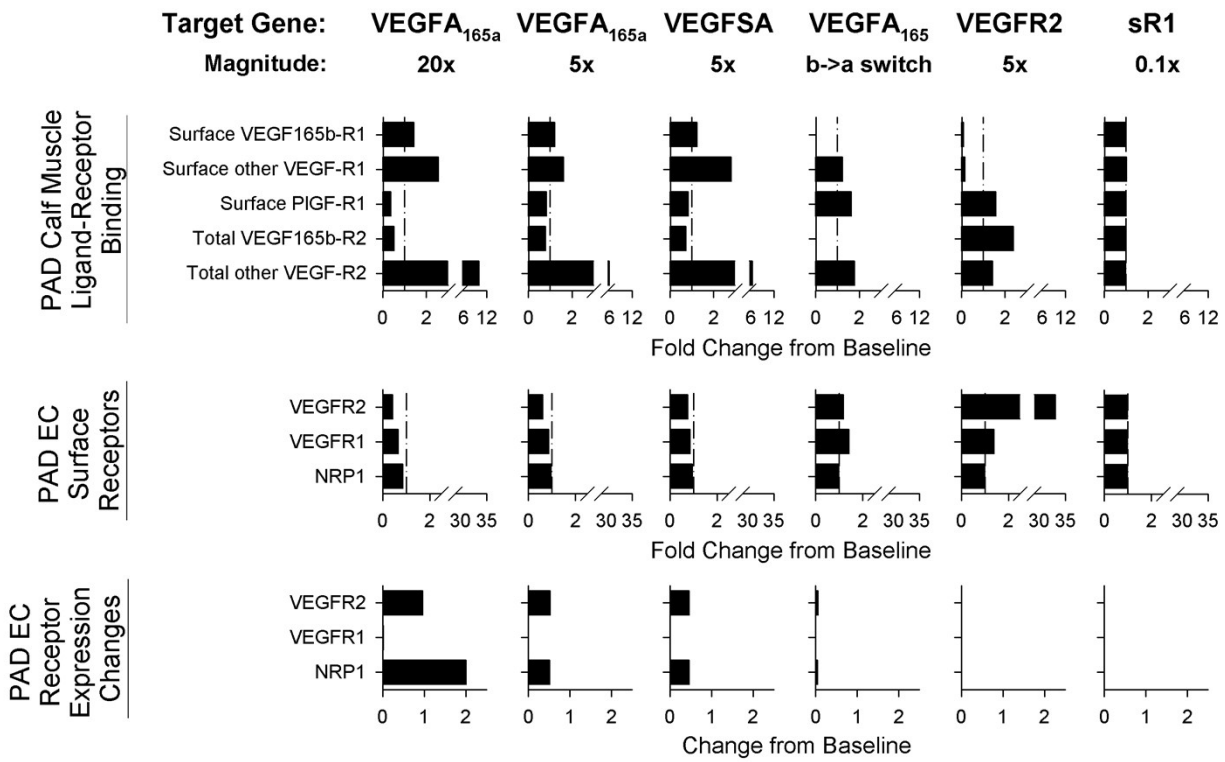

Fig S4. Additional metrics of response to gene therapy at Day 6 following treatment. This figure is related to **Fig. 3** of the main manuscript. Breakdown of ligands bound to VEGFR1 and VEGFR2 on endothelial cells (**top row**), endothelial surface receptor levels (**middle row**), and changes in receptor production required to hold total receptor levels constant 6 days post-treatment (**bottom row**).

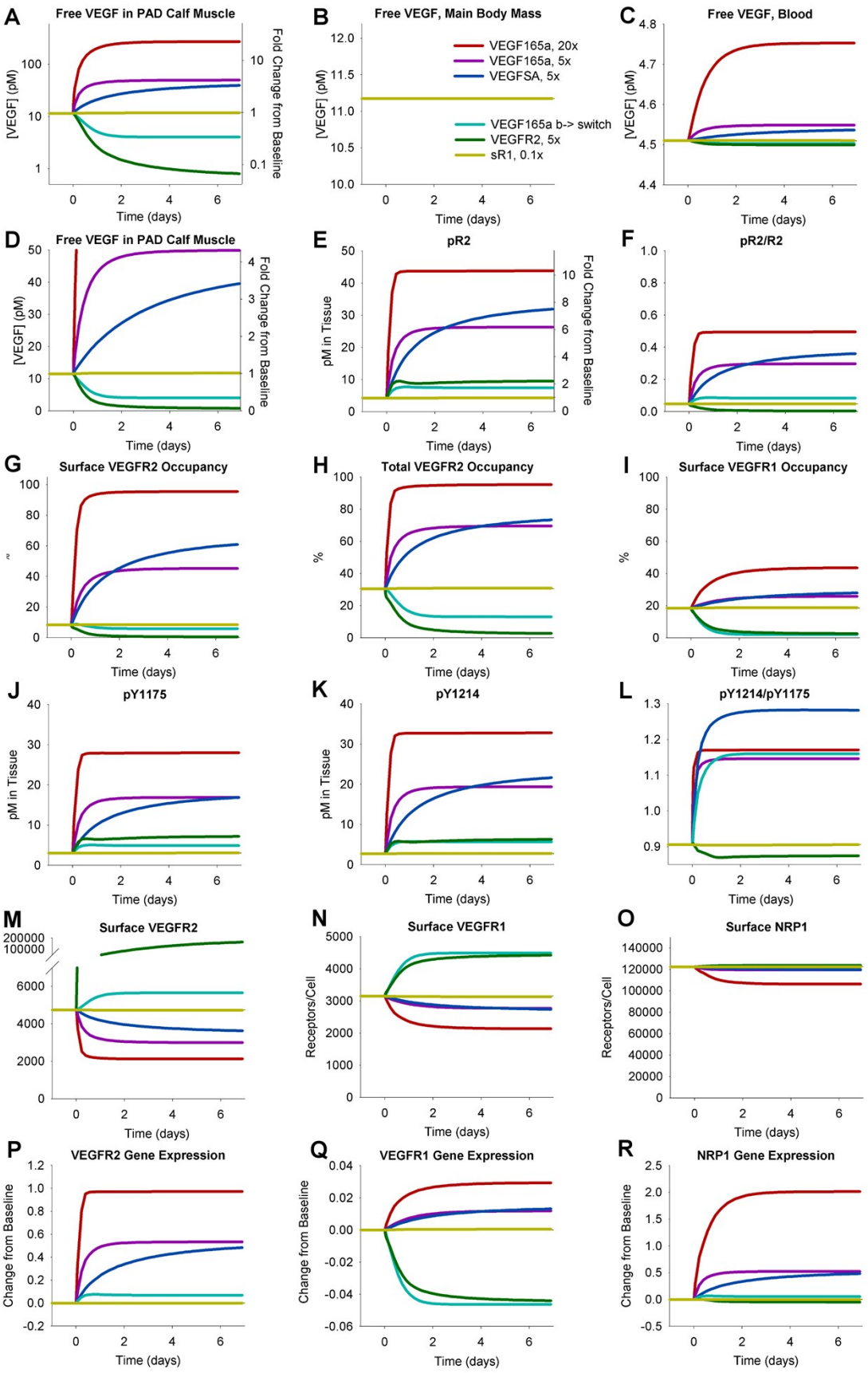
A
Free VEGF in PAD Calf Muscle
[VEGF] (pM)
Fold Change from Baseline
Time (days)
B
Free VEGF, Main Body Mass
VEGF165a, 20x
VEGF165a, 5x
VEGFSA, 5x
VEGF165a b-> switch
VEGFR2, 5x
sR1, 0.1x
[VEGF] (pM)
Time (days)
C
Free VEGF, Blood
[VEGF] (pM)
Time (days)
D
Free VEGF in PAD Calf Muscle
[VEGF] (pM)
Fold Change from Baseline
Time (days)
E
pR2
pM in Tissue
Fold Change from Baseline
Time (days)
F
pR2/R2
Time (days)
G
Surface VEGFR2 Occupancy
%
Time (days)
H
Total VEGFR2 Occupancy
%
Time (days)
I
Surface VEGFR1 Occupancy
%
Time (days)
J
pY1175
pM in Tissue
Time (days)
K
pY1214
pM in Tissue
Time (days)
L
pY1214/pY1175
Time (days)
M
Surface VEGFR2
Time (days)
N
Surface VEGFR1
Receptors/Cell
Time (days)
O
Surface NRP1
Receptors/Cell
Time (days)
P
VEGFR2 Gene Expression
Change from Baseline
Time (days)
Q
VEGFR1 Gene Expression
Change from Baseline
Time (days)
R
NRP1 Gene Expression
Change from Baseline
Time (days)

Fig S5. Detailed time-course response to gene therapy strategies. This figure is related to **Fig. 3** of the main manuscript. Free VEGF levels in other compartments (**A-D**), details of VEGFR2 phosphorylation (**E-F,J-L**), endothelial receptor occupancy (**G-I**), changes in surface receptor levels following treatment (**M-O**), and the dynamic changes in receptor production required to hold total receptor levels constant following treatment (**P-R**).

Fig S6. An
VEGF-targ
Concentrat
the Main B
IV infusion
rates in the
antibody a
only local \

effects become important (i.e. the concentrations of $VEGF_{165a}$ and $VEGF_{165b}$ in the other tissue compartment affect local VEGF levels). Changes in flow directions between compartments also occur following antibody treatment. Note that $VEGF_{165b}$ distribution is similarly impacted by both anti-$VEGF_{165b}$ and anti-VEGF; the difference in effect arises from the concomitant redistribution of $VEGF_{165a}$ by anti-VEGF.

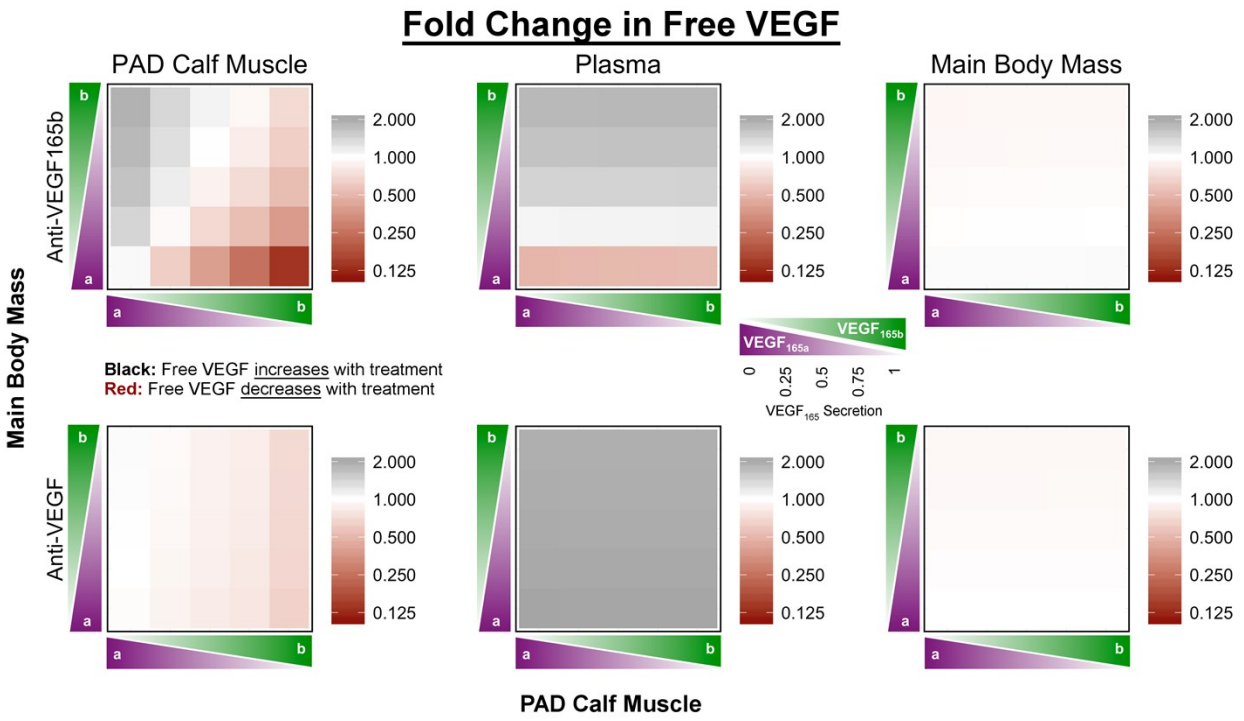

Fig S7. Effect of VEGF-targeting antibodies on systemic free VEGF distribution. This figure is related to **Fig. 5** of the main manuscript. Predicted fold change from baseline of total free VEGF in the PAD Calf Muscle (**left**), blood (**middle**) and Main Body Mass (**right**) on Day 6 following treatment with anti-$VEGF_{165b}$ (**top row**) or non-isoform-specific anti-VEGF (**bottom row**), as a function of the local fractional secretion of $VEGF_{165b}$ in the PAD Calf Muscle (x-axis) and the Main Body Mass (y-axis). Black indicates an increase in free VEGF, while red indicates a decrease.

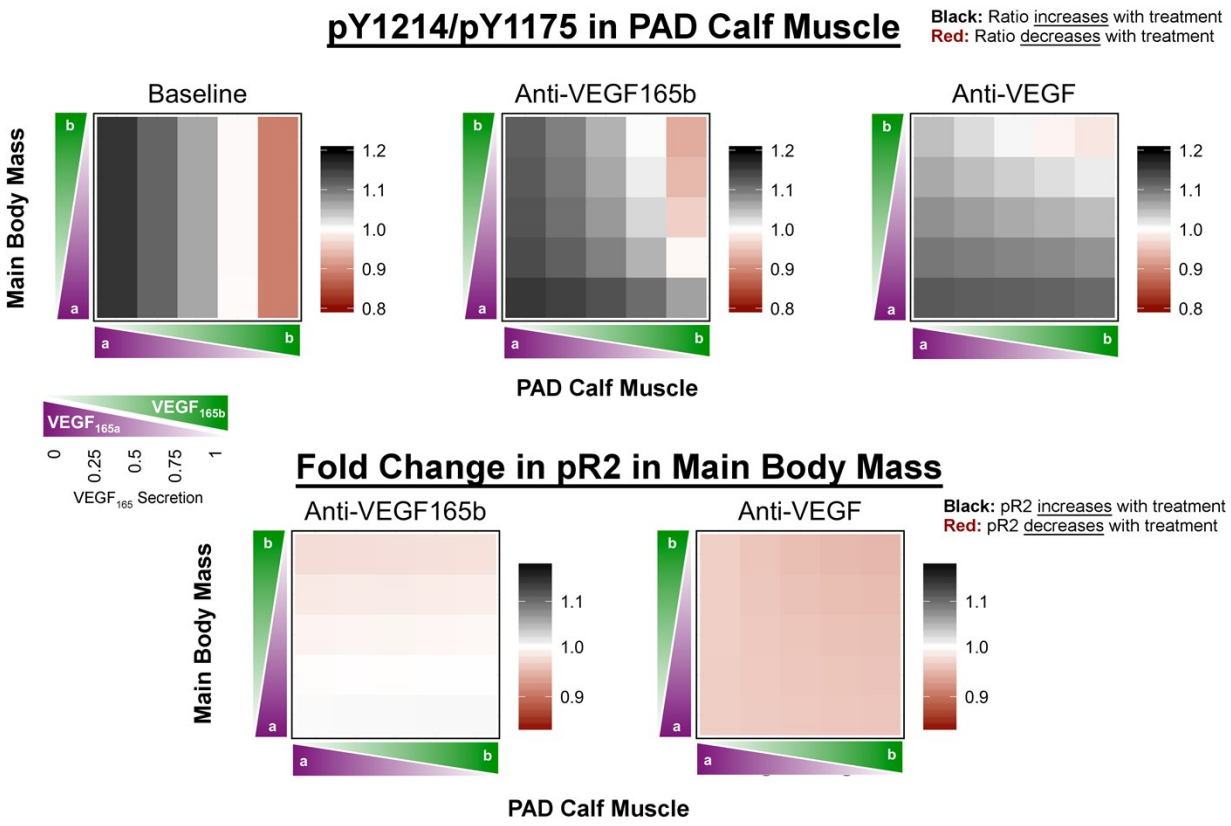

Fig S8. Additional effects of VEGF-targeting antibodies on endothelial VEGFR2 signaling *in vivo*. This figure is related to **Fig. 6** of the main manuscript. **Top:** Predicted ratio of VEGFR2 phosphorylation on Y1214 to Y1175 in the PAD Calf Muscle at baseline (**left**), and on Day 6 following treatment with Anti-$VEGF_{165b}$ (**middle**) or a non-isoform-specific Anti-VEGF (**right**), as a function of the local fractional secretion of $VEGF_{165b}$ in the PAD Calf Muscle (x-axis) and the Main Body Mass (y-axis). **Bottom:** Predicted fold change in VEGFR2 phosphorylation in the Main Body Mass on Day 6 following systemic antibody treatment. Black indicates an increase, while red indicates a decrease.

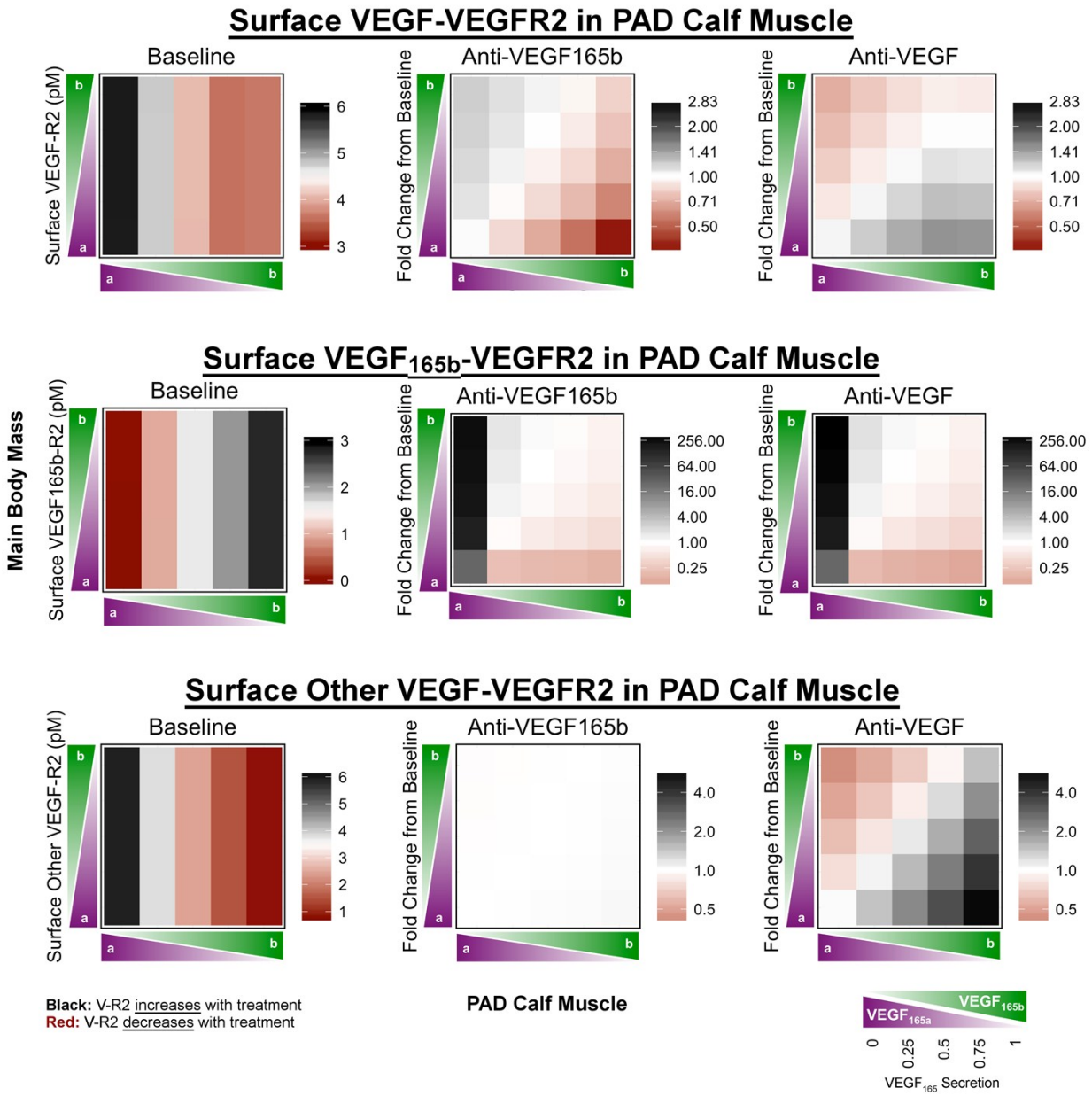

Fig S9. Effects of VEGF-targeting antibodies on endothelial total VEGFR2 ligation *in vivo*. This figure is related to **Fig. 6** of the main manuscript. Predicted total binding of VEGF to VEGFR2 (**top row**), $VEGF_{165b}$-R2 (**middle row**), and binding of other VEGF isoforms to VEGFR2 (**bottom row**) in the PAD Calf Muscle at baseline (**left**), and fold change from baseline on Day 6 following treatment with Anti-$VEGF_{165b}$ (**middle**) or a non-isoform-specific Anti-VEGF (**right**), as a function of the local fractional secretion of $VEGF_{165b}$ in the PAD Calf Muscle (x-axis) and the Main Body Mass (y-axis). Black indicates an increase, while red indicates a decrease. Note differences in color scales by row.

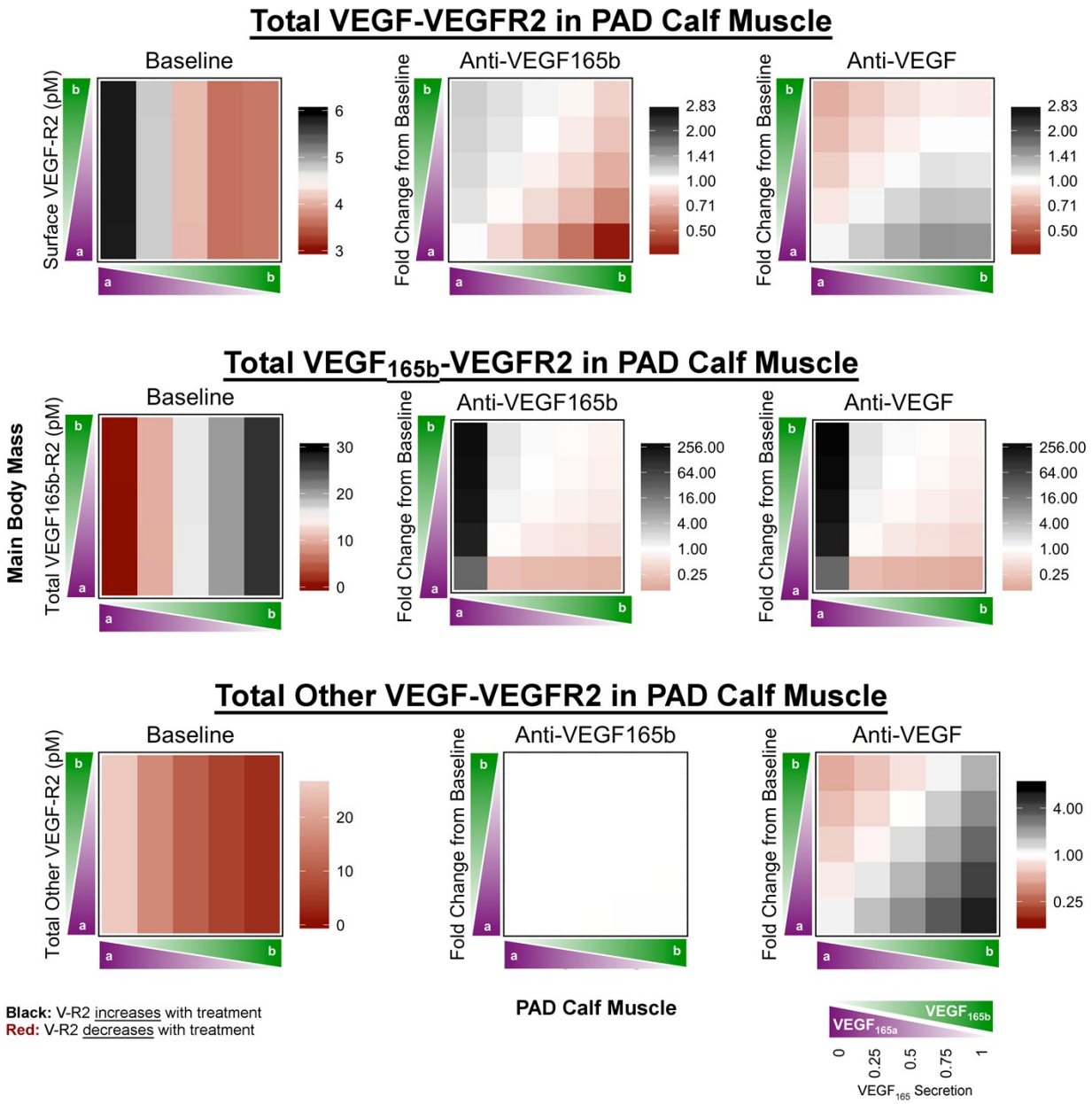

Fig S10. Effects of VEGF-targeting antibodies on endothelial cell surface VEGFR2 ligation *in vivo*. This figure is related to **Fig. 6** of the main manuscript. Predicted total binding of VEGF to VEGFR2 (**top row**), $VEGF_{165b}$-R2 (**middle row**), and binding of other VEGF isoforms to VEGFR2 (**bottom row**) in the PAD Calf Muscle at baseline (**left**), and fold change from baseline on Day 6 following treatment with Anti-$VEGF_{165b}$ (**middle**) or a non-isoform-specific Anti-VEGF (**right**), as a function of the local fractional secretion of $VEGF_{165b}$ in the PAD Calf Muscle (x-axis) and the Main Body Mass (y-axis). Black indicates an increase, while red indicates a decrease. Note differences in color scales by row. **Note:** Changes in total other VEGF binding to VEGFR2 following anti-$VEGF_{165b}$ treatment (bottom row, center) <1% (due to lack of competition between VEGF isoforms for binding to VEGFR2), which are not visible with the given scale.

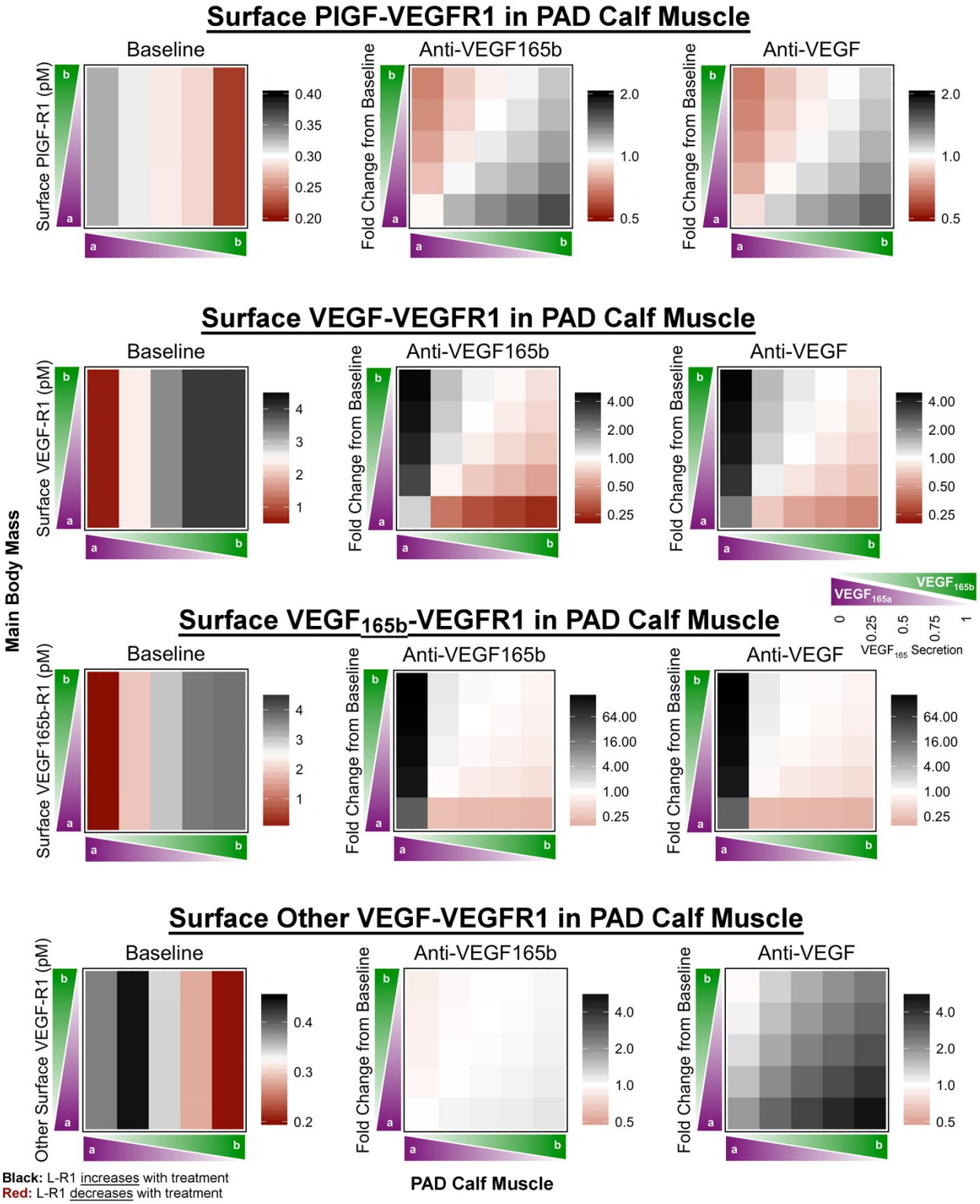

Fig S11. Effects of VEGF-targeting antibodies on endothelial cell surface VEGFR1 ligation *in vivo*. This figure is related to **Fig. 6** of the main manuscript. Predicted total binding of PlGF to VEGFR1 (**top row**), total VEGF to VEGFR1 (**2nd row**), $VEGF_{165b}$-R1 (**3rd row**), and binding of other VEGF isoforms to VEGFR1 (**bottom row**) in the PAD Calf Muscle at baseline (**left**), and fold change from baseline on Day 6 following treatment with Anti-$VEGF_{165b}$ (**middle**) or a non-

isoform-specific Anti-VEGF (**right**), as a function of the local fractional secretion of $VEGF_{165b}$ in the PAD Calf Muscle (x-axis) and the Main Body Mass (y-axis). Black indicates an increase in Free VEGF, while red indicates a decrease. Note differences in color scales by row.

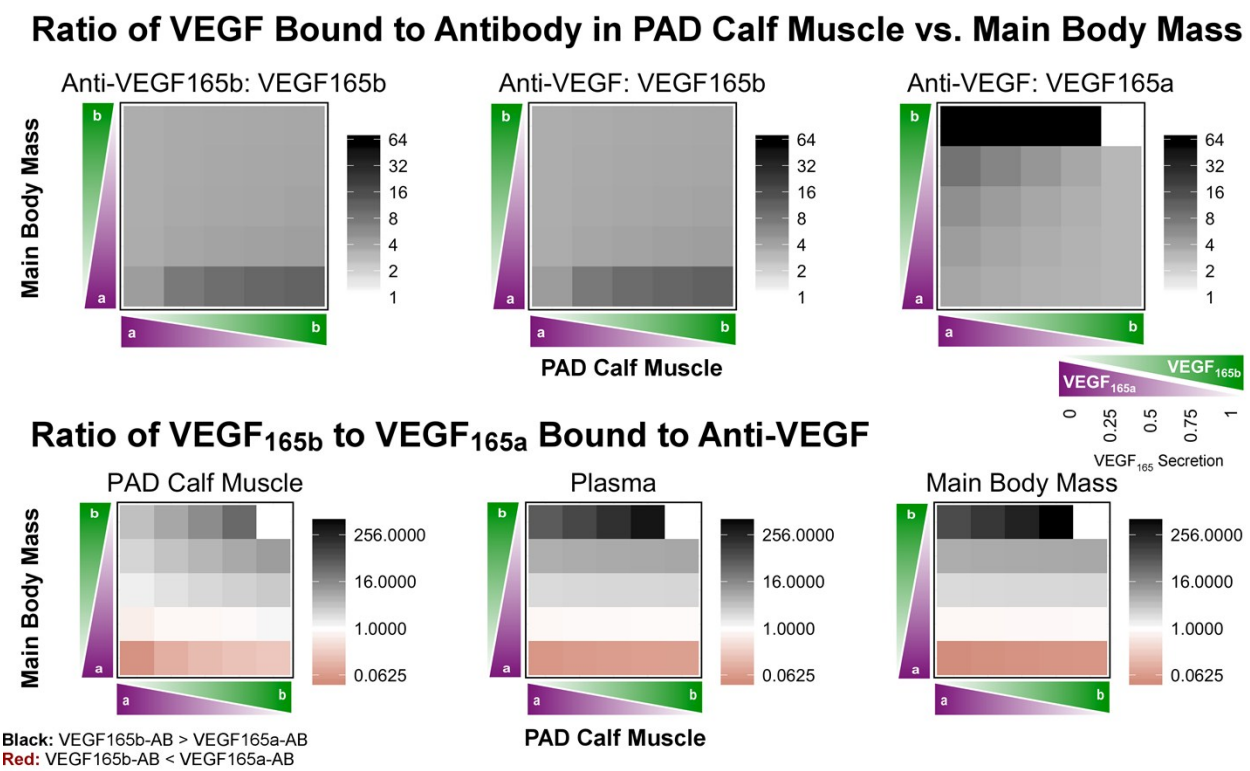

Fig S12. Relative antibody binding to $VEGF_{165a}$ and $VEGF_{165b}$ in the Main Body Mass and PAD Calf Muscle. This figure is related to **Fig. 5** of the main manuscript. **Top:** Predicted ratio of VEGF bound to the antibody in the PAD Calf Muscle as compared to the Main Body Mass on Day 6 following treatment, as a function of the local fractional secretion of $VEGF_{165b}$ in the PAD Calf Muscle (x-axis) and the Main Body Mass (y-axis). Left: $VEGF_{165b}$ bound to Anti-$VEGF_{165b}$; Middle: $VEGF_{165b}$ bound to Anti-VEGF; Right: $VEGF_{165a}$ bound to Anti-VEGF. **Bottom:** Predicted ratio of $VEGF_{165b}$ to $VEGF_{165a}$ bound to Anti-VEGF in the PAD Calf Muscle (**left**), Blood (**middle**), and Main Body Mass (**right**) at Day 6 following treatment. In most cases, $VEGF_{165b}$ dominates due to its over-representation relative to its secretion fraction. Black indicates a ratio >1, while red indicates a ratio <1.

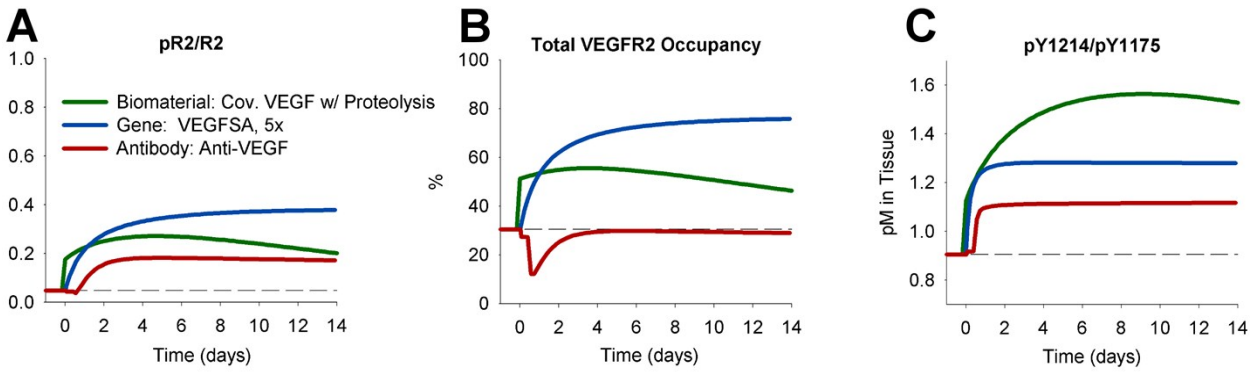

Fig S13. Comparison of VEGFR2 activation following biomaterial-based protein delivery, gene therapy, or anti-VEGF treatment. This figure is related to **Fig. 7** of the main manuscript. Fraction of total VEGFR2 phosphorylated (**A**), total VEGFR2 occupancy (**B**), and pY1214/pY1175 (**C**) over time following treatment induction.

Supplemental References

1. Kut C, Mac Gabhann F, Popel AS. Where is vegf in the body? A meta-analysis of vegf distribution in cancer. *British Journal of Cancer*. 2007;97:978-985